Generative Steady-State Visual Evoked Potential Models

Chun-Shu Wei
Bioengineering
UCSD
La Jolla, CA 92037
cswei@sccn.ucsd.edu

Luca Pion-Tonachini
Electrical and Computer Engineering
UCSD
La Jolla, CA 92037
lucapton@gmail.com

Eddie Yocon Chung
Bioengineering
UCSD
La Jolla, CA 92037
eyc014@eng.ucsd.edu

Praopim Limsakul
Bioengineering
UCSD
La Jolla, CA 92037
praopim.lim@gmail.com

Abstract

Steady-state evoked potential (SSVEP) is a periodic cortical response induced by repeated visual stimuli. This study aims to generate visual evoked potential (VEP) and to simulate SSVEP using existing mathematical models. Assessment of the results will include accuracy of the VEP and SSVEP as a temporal process as well as accuracy of the power spectrum for various input frequencies. The quantitative prediction of SSVEP is a pathway to understand the unexplained properties of SSVEP, and may provide useful information for future SSVEP-based practical applications.

1 Introduction

1.1 Cerebral Cortex

The cerebral cortex is the outermost layered structure of neural tissue of the brain in humans and some other vertebrates. It plays a key role in memory, perceptual awareness, thought, language, and consciousness.

The cerebral cortex can be divided into two major parts: Allocortex and neocortex. Neocortex is commonly believed to be the organ of thinking. It is the part of the mature cerebral cortex with six distinct layers, each layer contains a characteristic distribution of neuronal cell types and connections with other cortical and subcortical regions (figure1) [1], [2].

Layer 1, the molecular layer, consists mainly of extensions of apical dendritic tufts of pyramidal neurons and horizontally oriented axons, as well as glial cells [3]. It contains almost no neuron cell bodies. Layer 2 contains many small densely-packed pyramidal neurons which receive inputs from other cortical layers. Layer 3 contains medium-sized pyramidal neurons which send outputs to other cortical areas. Layer 4 receives inputs from outside the cortex [4]. Layer 5 contains the largest pyramidal neurons, which send outputs to the brainstem and spinal cord (the pyramidal tract). Layer 6 consists of pyramidal neurons and neurons with spindle-shaped cell bodies. Most cortical outputs leading to the thalamus

originate in layer 6, whereas most outputs to other subcortical nuclei originate in layer 5.

Sensory inputs first activate neurons in layer 4, which propagate the excitement up to layers 2 and 3, and from there down to layers 5 and 6. The organization of these connections into vertical columns, have led to models of the cortex in which billions of cortical columns act as the functional units. Most of the axons in the neocortex connect pyramidal neurons with other pyramidal neurons. Non-pyramidal neurons in the neocortex are referred to collectively as interneurons. Most of these interneurons (smooth stellate, basket cells, chandelier cells and double bouquet cells) use the inhibitory neurotransmitter gamma-amino butyric acid (GABA) [5].

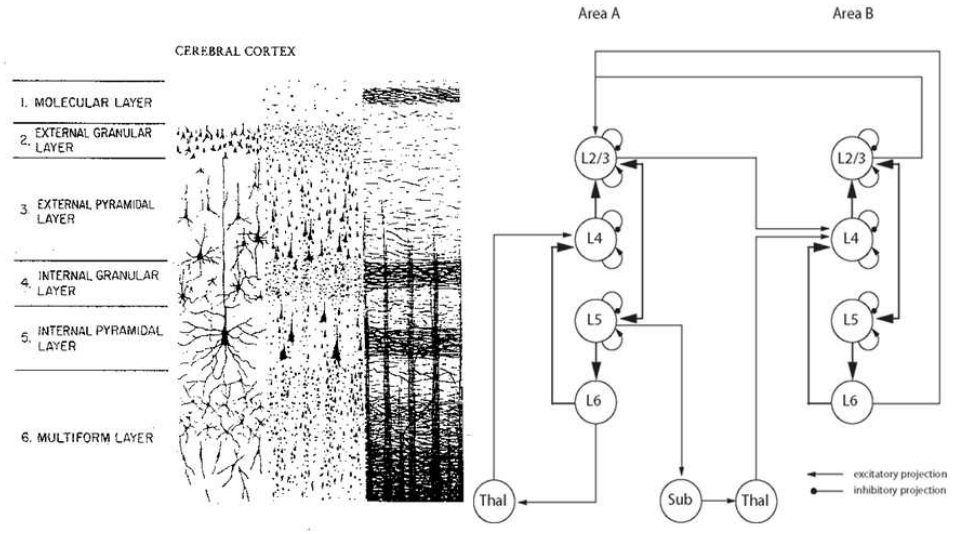

Figure 1: The layer structure of cerebral cortex and relationships between different cortical layers and columns

1.2 Visual evoked potential

A visual evoked potential (VEP) is an evoked electrophysiological potential following presentation of a visual stimulus. VEPs are used primarily to measure the functional integrity of the visual pathways from retina via the optic nerves to the visual cortex of the brain. Any abnormality that affects the visual pathways or visual cortex in the brain can affect the VEP. There are many ways to generate VEP, commonly used ways are strobe flash, flashing light-emitting diodes (LEDs), transient and steady state pattern reversal and pattern onset/offset. Since VEP can also be elicited by other stimuli, like walking, the commonly used way to extract VEP from background EEG activity is by signal averaging. The typical pattern after signal averaging is shown in figure 2. The nomenclature of the pattern is determined by using capital letters stating whether the peak is positive (P) or negative (N) followed by a number which indicates the average time for the event happens after specific pulse [6]. In typical VEP pattern there is a prominent negative component at peak latency of about 70 ms, a larger positive component at about 100 ms and a negative component at about 140 ms [7].

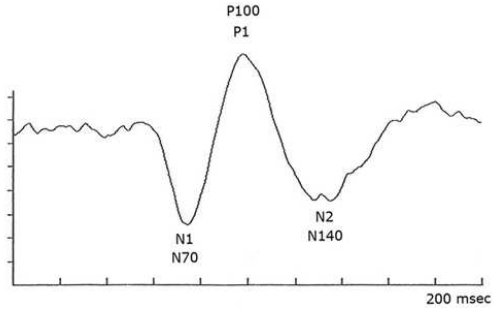

Figure 2: The typical VEP response

1.3 Visual evoked potential

Steady State Visually Evoked Potentials (SSVEP) are signals that are natural responses to visual stimulation at specific frequencies. When the retina is excited by a visual stimulus ranging from 3.5 Hz to 75 Hz, the brain generates electrical activity at the same frequency of the visual stimulus. The advantage to study SSVEP is it's high signal-to-noise ratio that helps researcher to find meaningful signals from noise. It is believed that SSVEP can be explained by the superpositioning of transient VEP.

1.4 Neuro mass model

Among the neuron modeling history, there are generally two kinds of neuron models, each has its distinct biological perspectives to develop neuro mass models. They are Morris and Lecar's model and Jansen's model. In Morris and Lecar's model, it considers single neuron cell's electrophysiological properties, for example diffusion of ions, properties of gap junctions...etc, while in Janson's model it focus on whole cortical columns [8], with sigmoidal functions to transform the average density of presynaptic firing arriving at the population into the average postsynaptic membrane potential (PSP). In this study we use Jansen's Model as a base to simulate VEP and SSVEP [9].

2 Methods

2.1 Cortical Column Model

In this work, we use the cortical column model from [9]. This model can be separated into two parts; single column, and two-column model.

Single column model consists of a group of neurons, including pyramidal cells (PYs), excitatory and inhibitory interneurons (INs) in one cortical column (figure 3A). Each neuron population receives the PSPs that are converted into an average pulse density of spike by a sigmoidal function (Eq.1) where $2e_0$ is the maximum firing rate, and v_0 is the PSP for which 50% firing rate is achieved, and r is the steepness of sigmoid function. The second transformation occurs when the average action potential entering a population is converted into the PSPs by means of linear transformation (Eq.2) with the impulse response $h_e(t)$ and $h_i(t)$ for the excitatory and the inhibitory case, respectively. The constant A and B limit the maximum amplitude of the PSPs, as well as, a and b are lumped parameters.

$$Sigm(v) = \frac{2e_0}{1 + e^{r(v_0 - v)}} \tag{1}$$

$$h_e = \begin{cases} Aat \cdot e^{-at} & ; \quad t \geq 0 \\ 0 & ; \quad t < 0 \end{cases} \quad and \quad h_i = \begin{cases} Bbt \cdot e^{-bt} & ; \quad t \geq 0 \\ 0 & ; \quad t < 0 \end{cases} \tag{2}$$

The interaction between the different populations is described by connectivity constants, Ci, which represents the average number of synaptic constant. The input of the system p(t) is the square pulse wave with various frequencies; while, the output is the result of excitatory and inhibitory synapse acting on the PYs. Therefore, the difference between $y_1(t) - y_2(t)$ represents a good approximation to the EEG signal [10]. Each PSP population introduces two non-linear, secondary differential equations of the form:

$$\ddot{y}(t) = Aa \cdot x(t) - 2a \cdot \dot{y}(t) - a^2 \cdot y(t) \tag{3}$$

which can be rewritten as first-order differential equations.

$$\dot{y}(t) = z(t) \quad and \quad \dot{z}(t) = Aa \cdot x(t) - 2a \cdot z(t) - a^2 \cdot y(t) \tag{4}$$

where $x(t)$ and $y(t)$ are the input and output signals, respectively.

According to Jansen and Rit [9], VEP components are caused the interaction between two or more cortical columns. For the two column model (figure 3B), the interaction between two columns is described via the connectivity constant K_1 and K_2 which control the synaptic strength, and the delay time constant a_d.

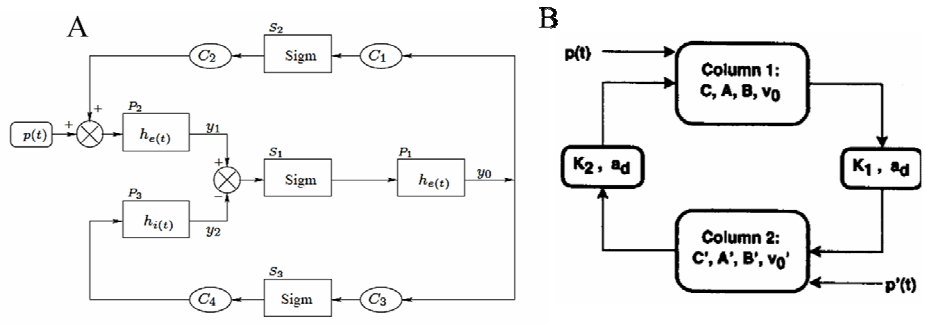

Figure 3: The schematic diagram of single column model (A), and two-column model (B) [9].

2.2 The thalamic-cortical model

The thalamic-cortical (TC) model consists of the thalamic module and the cortical module (see figure 4). This model describes the connection between thalamus and cortex.

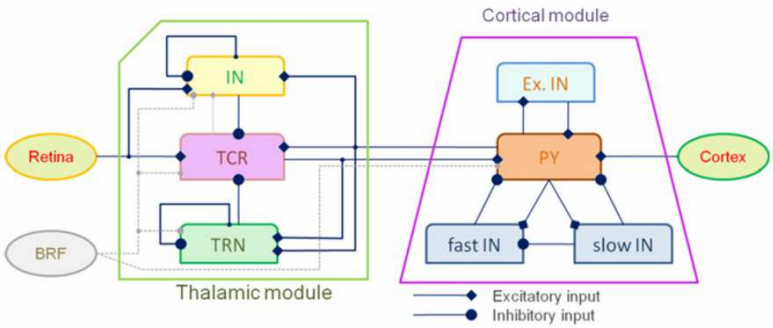

Figure 4: The general diagram of TC model [11].

The thalamic module consists of an excitatory group Thalamic Relay cells (TCR) and inhibitory group Interneurons (IN). The input signal (square pulse wave) from retina and backward connection from cortical PYs make excitatory synapses with TRC. However, the IN cells and the Thalamic Reticular Nucleus (TRN) cells send inhibitory feedback to the TCR cells [11].

For the cortical model, the concept is similar as Jansen's model; however, inhibitory interneurons are separated into two groups with slow synaptic kinetics and faster synaptic kinetics. The input *p(t)* is from the basal stochastic activity within the column. The cortical column also receives excitatory afferences from TCR relay neurons [10].

2.3 Simulated Visual Stimulation

A 100ms-long square pulse was applied as the input for VEP simulation using both Jansen and TC model. For SSVEP simulation, a 4s-long input signal was generated by a frame-based method proposed by Wang et al [12]. The flickering light source is simulated by periodic square pulses with various frequencies ranging from 1 through 40 Hz.

3 Results

3.1 Jansen's Model

The VEP reproduced by Jansen's model is not altogether accurate it consists of only a positive spike. When the frequency control parameter is set to two, it does have the P100 but lacks both the N75 and N135. When the frequency control parameter is varied, the rise and fall become faster as it increases.

While the SSVEP response of the two column Jansen's model is largely determined by the input frequency of the square wave and the frequency parameter, the output can still be generalized as pertaining to two distinct regimes, as well as a third transitory regime. The first occurs when the input frequency is slow enough that the model can respond to the rises and falls of the square wave in time allowing them to be phase locked. In the transitory regime, the rises and falls of the output fall very far behind that of the input. Rather than simply rising and falling at a slower rate, the output rises and falls once or twice (depending on the settings) and then fails to rise all together for a duration. In the third regime, there is no rise or fall as in the first. Instead the third resembles the noisy baseline that occurred when the output failed to rise in the transitory regime. Notably, that signal is still phase locked to the input.

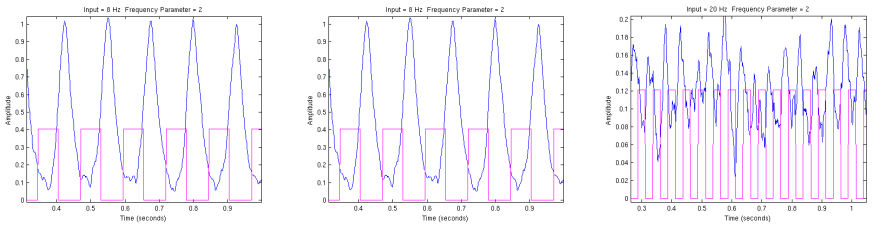

Figure 5: The time course of inputs and outputs with various input frequencies in Jansen's model.

The three regimes can be seen much more distinctly when viewing an image of the logarithmic power spectrum over all input frequencies. In the first regime there is a clearly defined fundamental harmonic. In the transitory regime the fundamental harmonic

diminishes in power a great deal (more so for higher values of the frequency control parameter). In the third regime the power spectrum is much more white though the fundamental harmonic is still visible.

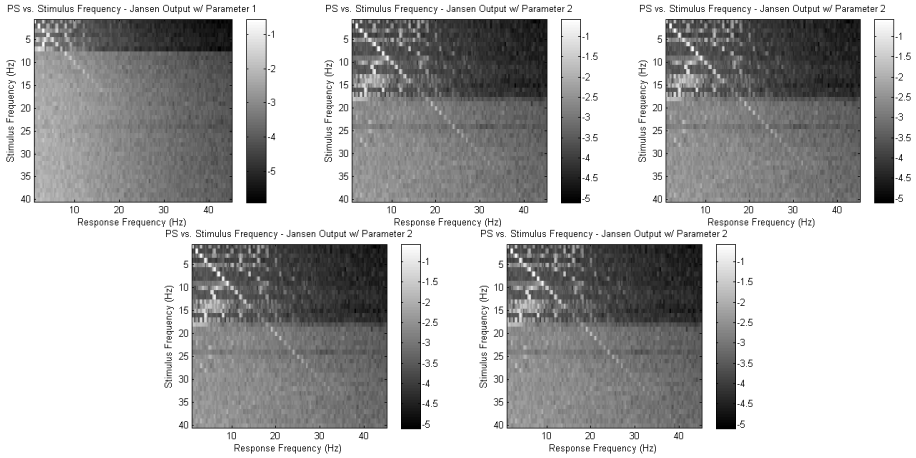

Figure 6: The power spectra of the SSVEP reproduced by Jansen's model with various parameters.

3.2 TC Model

The time course of VEP reproduced by TC model partly satisfies the characteristic of template VEP in experimental data. In the transient output response shown in figure 7, the negative and positive components (N80, P190, and N288) compose a waveform similar to the template except of the incorrect timing. The output time course presents an oscillation spindle with frequency around 5Hz during 2-3 seconds after the stimulation. The SSVEP simulation result reveals that TC model is able to reproduce the periodic oscillation waveform given periodic stimulation input.

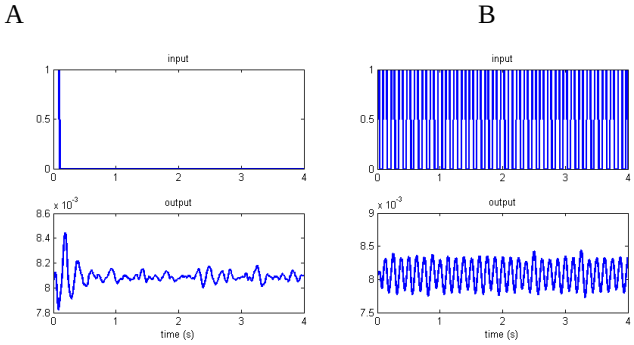

Figure 7: (A) The VEP induced by a single square pulse with 100ms in length. (B) The SSVEP induced by 10Hz stimulation.

The power spectra response of SSVEP generated by TC model shows obvious power peaks across all the fundamental frequencies corresponding to the stimulation. In addition, 5Hz oscillation can be observed given any stimulus frequency. There are first and second harmonics in the spectra, while subharmonics are not visible in this case. Unlike the case of Jansen's model, the spectral power at fundamental frequencies changes smoothly from low through high frequency.

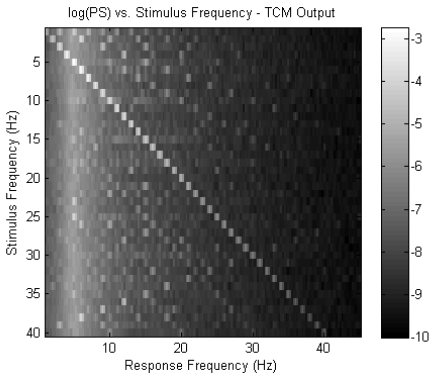

Figure 8: The logarithmic power spectra of SSVEP with stimulation frequency at 1 - 40 Hz.

4 Discussions

4.1 Jansen's Model

As a whole, the two column Jansen's model appears to be a much better at recreating the SSVEP power spectrum rather than recreating the actual time courses. The power spectrum produced by the model displays a strong fundamental harmonic as well as fairly strong superharmonics as well. What is truly impressive is that for lower input frequencies, the model even produces the subharmonic when there is none in the input signal.

The signal to noise ratio (SNR) of the fundamental harmonic also displays some properties found in experimental data. Wang el al. [13] found that the SNR had a lobe-like structure across stimulation frequencies. Jansen's model recreates a similar phenomenon above 10 Hz due to the diminished power in the fundamental harmonic during the transitory regime as well as far into the third regime. Below 10 Hz the real data showed lower SNR while our model had the highest SNR for low frequencies. One possible explanation for the variation at higher frequencies is that the lobed structure in the experimental data varies from subject to subject.

Another notable, though in this case negative, characteristic of this model is the lack of any frequency that maintains power throughout all input frequencies. The experimental data shows that power at 10 Hz is omnipresent and so having a similar phenomenon would have been beneficial to the model's credibility. There is some activity present at higher input frequencies when in the first regime that ranges from 5 Hz to 15 Hz depending on the frequency control parameter but it is not strong enough nor concentrated enough to be considered an accurate recreation.

The final notable problem with this model is the fact that the input noise on the second column has little to no nonlinear effect on the final output. That is to say, with the noise input removed, we are left with a very similar, denoised output. While this may simply be a characteristic of the model as we have built it, another possible explanation is that the feedback connection strengths between the columns may be too weak. As was previously described in the model section, the input to column two is noticeably weaker and therefore cannot endure the attenuation and still have enough power to affect the output beyond the first pass.

4.2 TC Model

The timing of the components in VEP varies across different species of animals. Previous study has shown the corresponding VEP components of primates, N40, P65, and N95 [14],

differs from the human VEP components. As the timing of VEP components varies from a species of animal to another, we regard TC model as a fair choice to simulate the cortical responses.

A B

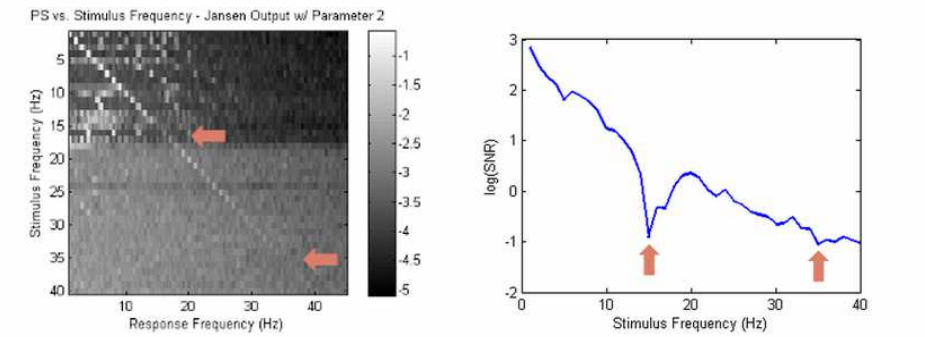

Figure 9: (A) The power spectra of SSVEP generated by Jansen's model with parameter 2. (B) The logarithmic SNR of along fundamental frequencies. The diminished power at 15 and 35 Hz are indicated by arrows.

A significance in TC model is that it successfully demonstrates the spontaneous oscillation that is independent to the stimulation frequency. This characteristic suggests that TC model is more powerful in mimicking the background rhythm which is often observed in EEG experiments. However, the 5Hz oscillation shown in power spectra is not coherent to the alpha oscillation that has stronger power around 10Hz. As the frequency of spontaneous oscillation may be regulated by the connection between the subunits in the model, it is worth optimizing the parameter set which may correctly generate alpha rhythm.

5 Conclusion

Both models have their strengths and weaknesses. Jansen's model recreates the harmonics and lobed SNR fairly well, whereas the TC model lacks these features. On the other hand, the TC model is much closer to reproducing the omnipresent alpha band power. In the future, we would like to combine these two models in hopes of maintaining the positive results of both while eliminating as many unrealistic characteristic of the models possible. This is feasible because the TC model is an advancement of Jansen's model such that they are both based on the same fundamental assumptions. One possible way to do this would be to add more cortical columns to the TC model connected in the way they were in Jansen's model.

Acknowledgments

The authors would like to thank Dr. Gert Cauwenberghs, Dr. Gabriel Silva and our TAs Bruno Umbria Pedroni and Chul Kim for their advice and suggestions for this project.

References

[1] Cerebral cortex. (2013) *Wikipedia, the free encyclopedia*

[2] Douglas, R. J., Martin, K. A. C., & Whitteridge, D. (1989) A Canonical Microcircuit for Neocortex. *Neural Computation*, 1(4), 480–488. doi:10.1162/neco.1989.1.4.480

[3] Shipp, S. (2007) Structure and function of the cerebral cortex. *Current Biology*, 17(12), R443–449.

doi:10.1016/j.cub.2007.03.044

[4] Jones, E. . (1998) Viewpoint: the core and matrix of thalamic organization. *Neuroscience*, 85(2), 331–345. doi:10.1016/S0306-4522(97)00581-2

[5] Best, B. (n.d.) *Basic Cerebral Cortex Function with Emphasis on Vision. Retrieved from http://www.benbest.com/science/anatmind/anatmd5.html*

[6] Evoked potential. (2013) *Wikipedia, the free encyclopedia*.

[7] Donnell J. Creel. (n.d.) *Visually Evoked Potentials.*

[8] Moran, R., Pinotsis, D. A., & Friston, K. (2013) Neural masses and fields in dynamic causal modeling. *Frontiers in Computational Neuroscience*, 7, 57. doi:10.3389/fncom.2013.00057

[9] Jansen, B. H., & Rit, V. G. (1995) Electroencephalogram and visual evoked potential generation in a mathematical model of coupled cortical columns. *Biological Cybernetics*, 73(4), 357–366. doi:10.1007/BF00199471

[10] Sotero, R. C., Trujillo-Barreto, N. J., Iturria-Medina, Y., Carbonell, F., & Jimenez, J. C. (2007) Realistically Coupled Neural Mass Models Can Generate EEG Rhythms. *Neural Computation*, 19(2), 478–512. doi:10.1162/neco.2007.19.2.478

[11] Bhattacharya, B. S., Coyle, D., & Maguire, L. P. (2011) A thalamo–cortico–thalamic neural mass model to study alpha rhythms in Alzheimer's disease. *Neural Networks*, 24(6), 631–645. doi:10.1016/j.neunet.2011.02.009

[12] Wang, Y., Wang, Y.-T., & Jung, T.-P. (2010) Visual stimulus design for high-rate SSVEP BCI. *Electronics Letters*, 46(15), 1057. doi:10.1049/el.2010.0923

[13] Wang, Y., Wang, R., Gao, X., & Gao, S. (2005) Brain-computer interface based on the high-frequency steady-state visual evoked potential. *2005 First International Conference on Neural Interface and Control, 2005. Proceedings* (pp. 37–39). doi:10.1109/ICNIC.2005.1499837

[14] Kraut, M. A., Arezzo, J. C., & Vaughan, H. G., Jr. (1985) Intracortical generators of the flash VEP in monkeys. *Electroencephalography and Clinical Neurophysiology*, 62(4), 300–312.